Magnetodielectric and magnetoelastic coupling in $TbFe_3(BO_3)_4$

U. Adem,[1] L. Wang,[1] D. Fausti,[2] W. Schottenhamel,[1] P. H. M. van Loosdrecht,[3] A. Vasiliev,[4] L. N. Bezmaternykh,[5] B. Büchner,[1] C. Hess,[1] and R. Klingeler[1,6]

[1]*Leibniz Institute for Solid State and Materials Research, IFW Dresden, Dresden, Germany*

[2]*Max Planck Group for Structural Dynamics, University of Hamburg-CFEL, Hamburg, Germany*

[3]*Zernike Institute for Advanced Materials, University of Groningen, Nijenborgh 4, 9747 AG Groningen, The Netherlands*

[4]*Moscow State University, Moscow 119992, Russia*

[5]*Kirensky Institute of Physics, Siberian Division, Russian Academy of Sciences, Akademgorodok, Krasnoyarsk 660036, Russia*

[6]*Kirchhoff Institute for Physics, University of Heidelberg, Heidelberg, Germany*

(Received 8 September 2009; revised manuscript received 18 July 2010; published 6 August 2010)

We have studied the magnetodielectric and magnetoelastic coupling in $TbFe_3(BO_3)_4$ single crystals by means of capacitance, magnetostriction, and Raman spectroscopy measurements. The data reveal strong magnetic field effects on the dielectric constant and on the macroscopic sample length which are associated to long-range magnetic ordering and a field-driven metamagnetic transition. We discuss the coupling of the dielectric, structural, and magnetic order parameters and attribute the origin of the magnetodielectric coupling to phonon mode shifts according to the Lyddane-Sachs-Teller relation.

DOI: 10.1103/PhysRevB.82.064406 PACS number(s): 77.84.−s, 75.30.Kz

I. INTRODUCTION

Many novel complex systems are investigated in the research on magnetoelastic and magnetodielectric coupling.[1–3] Among them, rare-earth iron borates $RFe_3(BO_3)_4$ constitute a family of noncentrosymmetrric oxides in which $4f$ moments are embedded in a network of $3d$ Fe spins. These compounds crystallize in trigonal $R32$ space group at high temperatures.[4,5] The members of the family having rare-earth elements with ionic radii smaller than Sm undergo a structural phase transition lowering the crystal symmetry from $R32$ to $P3_121$.[6,7] Based on single-crystal diffraction studies, it has been proposed that the structural transition results in an antiferroelectric state.[6] Magnetic exchange interactions for R=(magnetic) rare earths are complicated due to the $4f$-$3d$ interactions and the anisotropy of the $4f$ moments which, e.g., affects the direction of Fe spin in the ordered phase.

Structurally, $TbFe_3(BO_3)_4$ exhibits edge sharing FeO_6 polyhedra which are forming helicodial chains along the c axis.[5] Fe spins order antiferromagnetically at $T_N \approx 39$ K along the helicoidal chains of Fe atoms with the spins parallel to the hexagonal c axis while Tb moments are polarized from Fe ordering.[5,8–10] When a magnetic field is applied along the easy axis c, a field induced magnetic transition (FIMT) is observed at temperatures below T_N, i.e., there is a spin flop of the Fe spins while the Tb moments become fully aligned.

So far R=Gd, Pr, Nd, and Tb compounds have been studied in the context of multiferroics and magnetoelectrics. In fact, the space groups of both high- and low-temperature phases are not polar despite being noncentrosymmetric, therefore the family cannot be considered as multiferroic. On the other hand, it has been shown for R=Gd, Pr, Nd, and Tb that magnetic field induces electrical polarization, marking the materials as magnetoelectric.[11–14] Also, sizeable spin-lattice coupling was demonstrated for some of these compounds using magnetostriction measurements.[14,15] Within the family, the dielectric properties were reported only for R=Gd where the dielectric constant was found to decrease with decreasing temperature. The onset of magnetic ordering causes an anisotropic anomaly in ϵ. In the magnetically ordered phase Gd $4f$-Fe $3d$ magnetic interactions cause a spin-reorientation transition which is coupled to the dielectric constant via spin-lattice interaction.[7,16] Application of magnetic field strongly shifts the spin-reorientation transition, giving rise to 1% magnetodielectric effect.[16] Here, we present a detailed experimental study on the magnetodielectric and magnetoelastic coupling in $TbFe_3(BO_3)_4$. We have measured the dielectric constant and the magnetostriction and we show by analysis of Raman spectroscopy data that the magnetodielectric coupling is mediated by strain and caused by shifts in the corresponding transverse optical (TO)-phonon modes via Lyddane-Sachs-Teller (LST) relationship.

II. EXPERIMENTAL

The single crystals we used were from the same batch as in Ref. 8. The capacitance of the sample was measured using a homemade insert and Andeen-Hagerling AH2500A bridge in a 18 T Oxford cryostat between 5 and 300 K. The measurement frequency was 1 kHz. Magnetostriction measurements were carried out with a capacitance dilatometer[17] in the same cryostat and with the same capacitance bridge. Our dilatometer applies the tilted plate principle with the sample placed in the open center of a ringlike capacitor made from silver. It enables to follow the length changes in the sample at constant temperature upon changing the external magnetic field. The sample length was 1.23 mm. The field was changed quasistatically from 0 up to 14 T and back with a rate of 0.01 T/s. The length changes in the sample are calculated from the capacitance changes measured by a temperature stabilized capacitance bridge Andeen-Hagerling with a resolution of 5×10^{-7} pF. Thus, length changes of less than 0.01 Å can principally be resolved. Due to mechanical vibrations, the resolution is limited to 0.1–1 Å in practice.

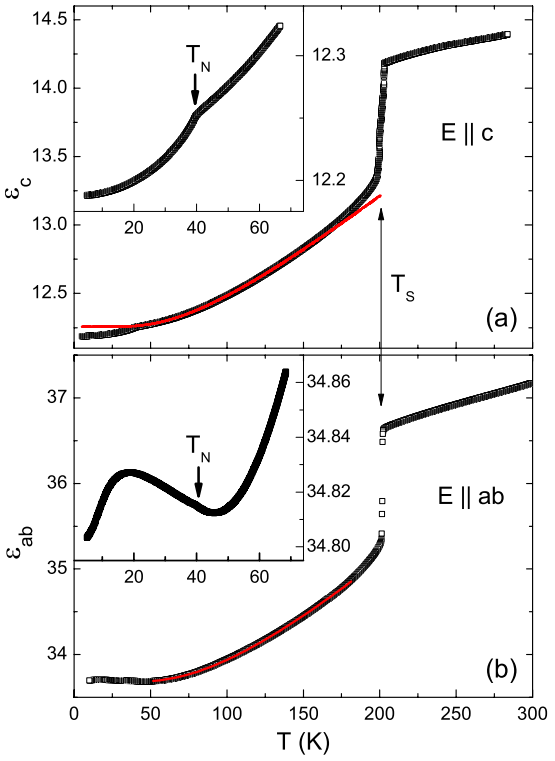

FIG. 1. (Color online) Temperature dependence of the dielectric constant of $TbFe_3(BO_3)_4$, for (a) $E \| c$ and (b) $E \perp c$. The insets highlight the data at low temperatures. The solid lines show fits according to Barrett's function (see the text).

The measurement frequency was 1 kHz. The field dependence of the magnetization up to 15 T was studied in a home-built vibrating-sample magnetometer.[18]

The Raman measurements were performed in a backscattering configuration, using a three-grating micro-Raman spectrometer (T64000 Jobin Yvon) equipped with a liquid nitrogen cooled charged coupled device detector. The frequency resolution was better than 2 cm^{-1} for the frequency region considered. The triple grating configuration allows the analysis of a broad spectrum from 10 000 down to 4 cm^{-1}. The sample was placed in an optical microscope cryostat. The temperature was varied from 4 to 55 K, with a stability of 0.1 K. The scattering was excited by the second-harmonic light of a Nd:YVO4 laser (532 nm), focused to 50 μm^2 with the power density on the sample kept below 0.1 $mW/\mu\, m^2$. The polarization was controlled both on the incoming and outgoing beams giving access to all relevant polarization combinations. The Raman measurements reported in the paper are performed with both the light's k vector and the polarization of the incoming and outgoing field in the BO_3 planes.

III. RESULTS AND DISCUSSION

Figure 1(a) shows the temperature dependence of the dielectric constant measured along the c axis. In the whole temperature regime under study, ϵ_c decreases upon cooling. In addition, we observe an abrupt decrease at the structural phase transition at $T_S = 202$ K. Also the magnetic ordering of the Fe spins at $T_N \approx 39$ K causes an anomaly in the dielectric constant [see the inset of Fig. 1(a)] which is however much smaller than that at T_S. The temperature dependence of the dielectric constant measured perpendicular to the c axis in general resembles the behavior for $E \| c$ but there are subtle differences at low temperature (Fig. 1). We again observe a discontinuity at T_S but unlike the case $E \| c$ there is only a very weak anomaly at T_N [cf. inset of Fig. 1(b)]. Instead, the data display a minimum above the magnetic ordering temperature, i.e., around 50 K, below which the dielectric constant increases. Upon further cooling, ϵ_{ab} decreases again below a broad maximum around 20 K.

The effect of an external magnetic field on ϵ_c applied parallel to the c axis is shown in Fig. 2(a). At $T = 5$ K, the capacitance is rather field independent for small $B \| c$ but a sharp increase appears around 4 T. At higher fields, the capacitance increases nearly linearly with a rather constant slope. The critical field of the jump in ϵ_c increases upon heating and the size of the jump becomes smaller. Above T_N, i.e., in absence of long-range magnetic order, the jump $\Delta\epsilon$ vanishes. Note that for all temperatures studied in the magnetically ordered phase the behavior in the high-field phase is nearly independent of temperature and the slope at high fields is very similar above T_N, too. The sharp anomaly in the dielectric constant is associated to a previously found FIMT which is clearly visible in magnetization measurements [see Fig. 2(b)].[8] The magnetization data show a huge jump of roughly $9\mu_B$/f.u. at the FIMT, and similar to the jump in ϵ the anomaly ΔM decreases and shifts to higher fields upon heating. The field induced magnetic transition is not only associated to jumps in ϵ_c and in the magnetization but it is also accompanied by strong magnetostrictive effects. As seen in in Fig. 2(c), the c axis exhibits a jumplike decrease at the critical field. Again, the jump reduces upon heating and it is restricted to the magnetically ordered phase. In general, the c axis contracts in the whole field range studied. In Fig. 2(d), the magnetic field dependence of ϵ_{ab} is shown, with the magnetic field again applied along the c axis. We again observe that the magnetic field dependence is small in both the low-field and the high-field antiferromagnetic phases while the largest changes occur at the FIMT. However, unlike the measurement for ϵ_c, the dielectric constant decreases with magnetic field in the field induced phase. The phase diagram shown in the inset summarizes the transition fields of the FIMT vs temperature as derived from dielectric constant, magnetization, magnetostriction, and specific heat.[8] We note that sharp changes in magnetostriction and electrical polarization at $T = 4.2$ K were reported recently in pulsed field studies, too.[14,15] The reported anomalies in the magnetostriction are however about two times smaller than found with our quasistatic setup which might be associated to the different experimental approach, i.e., pulsed magnetic field and usage of a piezoelectric sensor glued to the sample. In addition, there are also qualitative differences to our data, i.e., in $\Delta L_a/L_a$ at $B \| c > B_c$ and pronounced hysteresis effects in the magnetostriction and the electrical polarization.

To summarize the experimental data in Fig. 2, at the FIMT $TbFe_3(BO_3)_4$ displays a magnetically driven phase transition which is associated to sharp jumps in (1) the dielectric constant, (2) the magnetization, and (3) in the length

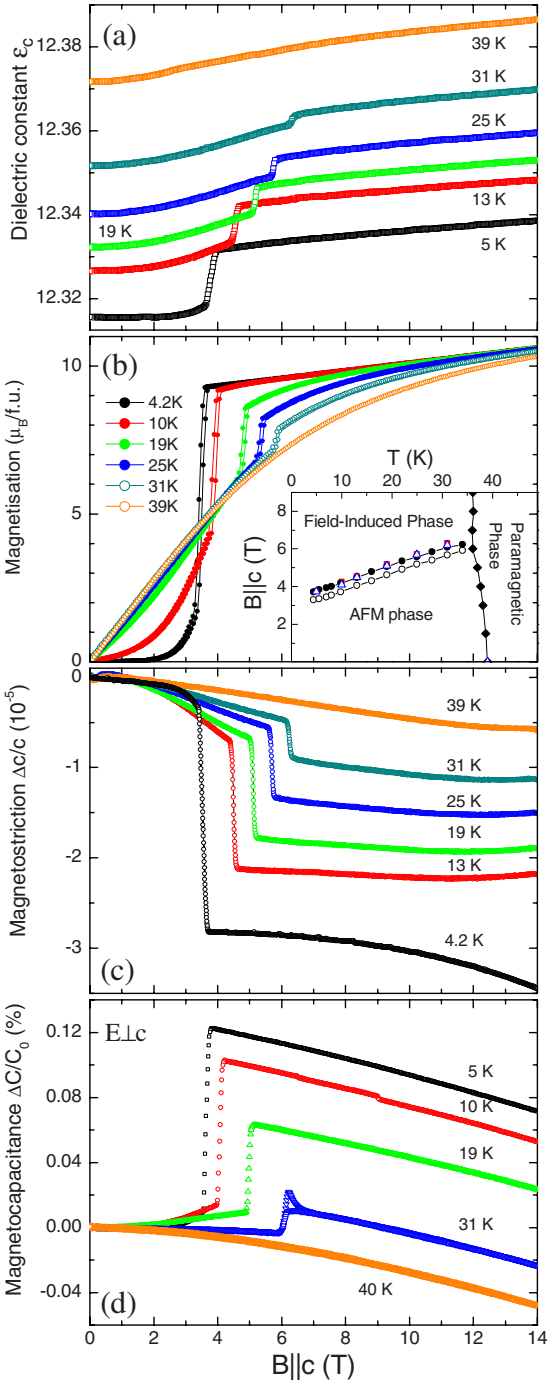

FIG. 2. (Color online) (a) The magnetic field dependence of the dielectric constant for $E\|c$ and $B\|c$, (b) magnetization (from Ref. 8), (c) magnetostriction of the c axis, and (d) capacitance for $E \perp c$ and $B\|c$. The inset displays the magnetic phase diagram derived from dielectric constant, magnetization, magnetostriction, and thermal-expansion studies.

of the c axis. It has been shown earlier for the magnetic degrees of freedom that, at the FIMT, there is a spin flop of the Fe spins accompanied by a magnetic flip of the Tb moments.[8]

The pronounced magnetoelastic coupling and the resulting jump of the sample length at the FIMT might suggest

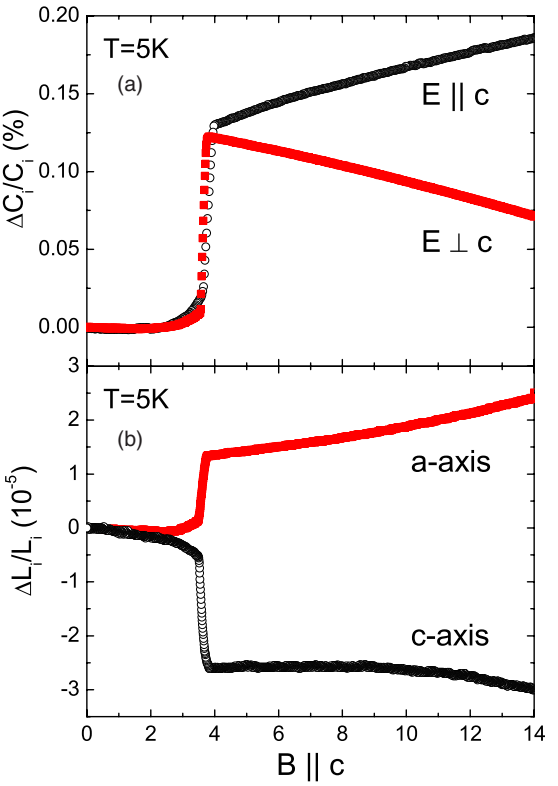

FIG. 3. (Color online) (a) Magnetocapacitance parallel and perpendicular to the c axis, and (b) magnetostriction along the a and c axes, respectively, of $TbFe_3(BO_3)_4$, at $T=5$ K, for magnetic fields applied along the c axis.

that the observed step in the dielectric constant is only associated to the magnetostriction, i.e.,

$$C = \epsilon_0 \epsilon \frac{A}{d}, \tag{1}$$

where ϵ_0 is the permittivity of the free space, ϵ is the dielectric constant, A is the area of the contacts, and d is the thickness of the sample. In general, a magnetic field induced jump in the sample length implies a capacitance anomaly which cannot be discussed in terms of the magnetodielectric effect. This scenario can however be clearly ruled out if the anisotropy of the magnetostriction and magnetocapacitance is considered (cf. Fig. 3). If a magnetic field is applied along the c axis, the length of the c axis and the a axis sharply shrinks and increases, respectively. Such an opposite sign of the length jumps is expected due to at least partial volume conservation of the magnetoelastic distortion. In contrast, both jumps in ϵ_c and ϵ_{ab} exhibit the same sign, i.e., magnetostriction has only a minor effect on the observed field dependence of ϵ and cannot explain the changes in $\epsilon(B)$. Therefore, the anomalies clearly point to a direct magnetodielectric coupling.

As discussed above, the general behavior of the dielectric constant vs temperature is rather isotropic while there is a weak difference between $\epsilon_c(T)$ and $\epsilon_a(T)$ at low temperatures. Interestingly, despite the fact that in $GdFe_3(BO_3)_4$ the magnetic structure in the ordered phase is different compared

to $TbFe_3(BO_3)_4$, the anomaly at T_N as well as the low-temperature behavior $\epsilon_c(T)$ and $\epsilon_{ab}(T)$ is roughly similar in both compounds.[16] In particular, both materials exhibit an increase in ϵ_{ab} below T_N which in $GdFe_3(BO_3)_4$ is truncated by a spin-reorientation transition. For $GdFe_3(BO_3)_4$, the upturn was suggested to originate from the polarization of Gd spins and the vicinity of a spin-reorientation transition.[16] In contrast, there is no spin-reorientation in $TbFe_3(BO_3)_4$ but as well the specific heat as the magnetization data exhibit a broad Schottky-type anomaly at the temperature where there is the peak in ϵ_{ab}. Recently, the anomalies of the specific heat and the magnetization were explained in terms of temperature-driven population of the ground state of Tb ion split by the internal field of Fe spins[8] which suggests a similar, i.e., Schottky type, scenario for the broad peak in ϵ_{ab}.

In the following we will discuss the origin of the observed magnetodielectric coupling. In general, the dielectric constant is related to optical-phonon frequencies via the Lyddane-Sachs-Teller relationship,

$$\epsilon_0 = \frac{\omega_L^2}{\omega_T^2}\epsilon_\infty. \tag{2}$$

In this equation ω_L and ω_T are the long-wavelength longitudinal and transverse optical-phonon mode frequencies, respectively. ϵ_0 is the static dielectric constant, i.e., the dielectric constant at zero frequency, and ϵ_∞ is the optical dielectric constant. Following the early literature on $BaMnF_4$,[19] MnO,[20] and MnF_2,[21] we have tried to relate the dielectric constant we measured to the relevant TO-phonon modes. In order to do so, we have used a modified Barrett equation as described in the aforementioned references as follows:

$$\epsilon(T) = \epsilon(0) + A/[\exp(\hbar\omega_0/k_BT) - 1]. \tag{3}$$

In this equation, A is a coupling constant and ω_0 is the mean frequency of the final states in the lowest lying optical-phonon branch. By fitting our data as indicated by the solid lines in Fig. 1 we obtained $A=33.6$, $\omega_0=206$ cm^{-1} for ϵ_{ab} and $A=12.2$, $\omega_0=177$ cm^{-1} for ϵ_c. We note the transverse optical mode that we obtained from the Barrett function fits corresponds to an average of all the contributing transverse optical modes in the respective direction.[21]

We have done Raman spectroscopy measurements to look for direct evidence of spin-lattice coupling. According to the previous reports[7,22] there are 59 transverse optical modes that correspond to ϵ_{ab}, i.e., phonon modes corresponding to a TO mode propagating perpendicular to the c axis. We have checked the temperature dependence of these modes and observed that only two low-lying ones shift their frequency at low temperatures: the first one at 200 cm^{-1} and the second one at 260 cm^{-1}. The modes at other frequencies do not significantly change their frequency. We show in Fig. 4(a) two representative low-lying phonon modes around 200 cm^{-1}. Upon cooling below the magnetic ordering temperature, one of the modes with the frequency 206 cm^{-1} does not shift with changing temperature while the frequency of the lower lying transverse phonon mode at 200 cm^{-1} is shifting remarkably at T_N. Its shift provides direct evidence for the spin-lattice coupling since exchange striction

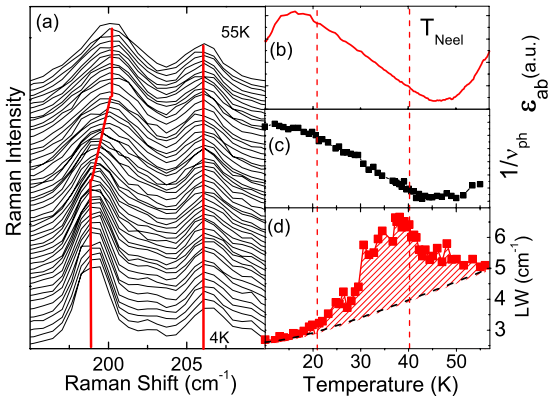

FIG. 4. (Color online) Comparison between the behavior of the phonon mode and the dielectric constant. (a) Temperature dependence of the phonon frequency responsible of the anomaly measured in the dielectric constant. (b) Dielectric constant measured perpendicular to the c axis. (c) Inverse of the phonon frequency as a function of temperature. (d) Linewidth of the phonon mode associated to the dielectric constant anomalous behavior.

stretches or elongates the bonds and hence shifts the phonon frequencies when magnetic ordering takes place.

The anomalous softening of the phonon mode reported in Fig. 4(a) is a possible reason for the behavior of the dielectric constant. Below the antiferromagnetic ordering temperature T_N, the behavior of the dielectric constant perpendicular to c (as discussed in the previous section) is rationalized in the light of the Raman response. As suggested by the LST equation the dielectric constant is inversely proportional to the frequency of the TO-phonon mode, associated to it. We note that usually LO modes and ϵ_∞ are assumed as temperature independent.[21,23] Figure 4 summarizes the qualitative agreement between (b) temperature dependence of the dielectric constant and (c) the inverse of the phonon frequency. Remarkably, the measured changes in the dielectric constant correspond very well to a decrease in the phonon frequency as described by the LST equation. We note however that in order to have a quantitative agreement, one needs to add the contributions from the all the relevant symmetry allowed TO modes.

In addition to this, the data imply a large anomalous broadening of the phonon mode at the magnetic transition itself. This is shown in Fig. 4(d) where the phonon linewidth as a function of temperature across the antiferromagnetic ordering temperature is presented. The black dashed line describes the expected decrease in the phonon lifetime as a function of temperature as if it was purely due to the usual phonon anharmonicity. The (red) dashed area in Fig. 4(d) reveals that in the temperature region close to the magnetic transition another decaying channel is available for the transverse optical mode. In the vicinity of the Neel temperature, the phonon broadening deviates much stronger from the expected behavior suggesting that a phonon-magnon coupling channel becomes active at the magnetic ordering temperature. This strongly suggests that the additional decaying channel reducing the phonon lifetime is not directly coupled to the magnetic order parameter but rather to its fluctuations.

In conclusion, we have demonstrated magnetodielectric coupling in $TbFe_3(BO_3)_4$ using capacitance measurements

and revealed the correlation between spin-phonon coupling and dielectric constant. We have shown that magnetodielectric coupling cannot be explained by the magnetostrictive effects but it occurs via shifting of the associated optical-phonon modes. The magnetic field induced phase transition the magnetic field induced phase transition is associated to sharp changes in not only the magnetic but also dielectric and structural degrees of freedom, i.e., the spin flop of Fe spins is accompanied not only by full polarization of the Tb moments but also to a significant distortion probably of the FeO_6 octaedra and a jump in the dielectric constant.

ACKNOWLEDGMENTS

We thank K. L. and S. G. for technical support. Work was supported by the DFG through Grants No. HE 3439/6 and No. 486 RUS 113/982/0-1.

[1] W. Eerenstein, N. D. Mathur, and J. F. Scott, Nature (London) **442**, 759 (2006).
[2] S. W. Cheong and M. Mostovoy, Nature Mater. **6**, 13 (2007).
[3] M. Fiebig, J. Phys. D **38**, R123 (2005).
[4] J. C. Joubert, W. B. White, and R. Roy, J. Appl. Crystallogr. **1**, 318 (1968).
[5] J. A. Campá, C. Cascales, E. Gutiérrez-Puebla, M. A. Monge, I. Rasines, and C. Ruíz-Valero, Chem. Mater. **9**, 237 (1997).
[6] S. A. Klimin, D. Fausti, A. Meetsma, L. N. Bezmaternykh, P. H. M. van Loosdrecht, and T. T. M. Palstra, Acta Crystallogr., Sect. B: Struct. Sci. **61**, 481 (2005).
[7] D. Fausti, A. A. Nugroho, P. H. M. van Loosdrecht, S. A. Klimin, M. N. Popova, and L. N. Bezmaternykh, Phys. Rev. B **74**, 024403 (2006).
[8] E. A. Popova *et al.*, Phys. Rev. B **75**, 224413 (2007).
[9] D. Volkov, E. Popova, N. Kolmakova, A. Demidov, N. Tristan, Y. Skourski, B. Buechner, I. Gudim, and L. Bezmaternykh, J. Magn. Magn. Mater. **316**, e717 (2007).
[10] C. Ritter, A. Balaev, A. Vorotynov, G. Petrakovskii, D. Velikanov, V. Temerov, and I. Gudim, J. Phys.: Condens. Matter **19**, 196227 (2007).
[11] A. K. Zvezdin, S. S. Krotov, A. M. Kadomtseva, G. P. Vorob'ev, Y. F. Popov, A. P. Pyatakov, L. N. Bezmaternykh, and E. A. Popova, JETP Lett. **81**, 272 (2005).
[12] A. M. Kadomtseva, Yu. F. Popov, G. P. Vorob'ev, A. A. Mukhin, V. Yu. Ivanov, A. M. Kuz'menko, and L. N. Bezmaternykh, JETP Lett. **87**, 39 (2008).
[13] A. K. Zvezdin, G. P. Vorob'ev, A. M. Kadomtseva, Y. F. Popov, A. P. Pyatakov, L. N. Bezmaternykh, A. K. Kuvardin, and E. A. Popova, JETP Lett. **83**, 509 (2006).
[14] A. K. Zvezdin, A. M. Kadomtseva, Y. F. Popov, G. P. Vorob'ev, A. P. Pyatakov, V. Y. Ivanov, A. M. Kuz'menko, A. A. Mukhin, L. N. Bezmaternykh, and I. A. Gudim, JETP **109**, 68 (2009).
[15] A. A. Demidov, N. P. Kolmakova, D. V. Volkov, and A. N. Vasiliev, Physica B **404**, 213 (2009).
[16] F. Yen, B. Lorenz, Y. Y. Sun, C. W. Chu, L. N. Bezmaternykh, and A. N. Vasiliev, Phys. Rev. B **73**, 054435 (2006).
[17] L. Wang *et al.*, Phys. Rev. B **80**, 094512 (2009).
[18] R. Klingeler, B. Büchner, K. Y. Choi, V. Kataev, U. Ammerahl, A. Revcolevschi, and J. Schnack, Phys. Rev. B **73**, 014426 (2006).
[19] D. L. Fox, D. R. Tilley, J. F. Scott, and H. J. Guggenheim, Phys. Rev. B **21**, 2926 (1980).
[20] M. S. Seehra and R. E. Helmick, Phys. Rev. B **24**, 5098 (1981).
[21] M. S. Seehra and R. E. Helmick, J. Appl. Phys. **55**, 2330 (1984).
[22] A. de Andres, F. Agullo-Rueda, S. Taboada, C. Cascales, J. Campa, C. Ruiz-Valero, and I. Rasines, J. Alloys Compd. **250**, 396 (1997).
[23] G. A. Samara and P. S. Percy, Phys. Rev. B **7**, 1131 (1973).